Deployable bundle modulus structures with reciprocal linkages for emergency buildings

J. Pérez-Valcárcel [*], M. Muñoz-Vidal, F. Suárez-Riestra, Isaac R. López-César, M.J. Freire-Tellado

Grupo de Estructuras Arquitectónicas (GEA). Estructuras singulares (GES), Dpto. de Tecnología de la Construcción, Escuela Técnica Superior de Arquitectura, Universidade da Coruña. Campus de A Coruña, Spain

ARTICLE INFO

ABSTRACT

Deployable structures are an ideal solution for emergency buildings because of their lightness and compactness, allowing them to be transported to wherever they are needed. Generally the most frequent solutions use Scissor-like-Elements (SLE), but in this case the use of bundle modules is proposed. These systems were developed by Pérez Piñero, but have hardly been used since then. The article analyses the problems they present, as well as their advantages in reducing the number of bars and linkages required, which allows for the design of simpler and more economical structures. The geometrical and mechanical conditions of the linkages for triangular and square modules are analysed, as well as the typologies that may arise. A calculation method is also developed to analyse this type of structure. Finally, the performance of a flat grid is analysed in an analytical and experimental way using reciprocal links at its ends. Both theoretical calculations and experimental tests allow us to demonstrate the viability and efficiency of this new type of structure.

1. Introduction

Deployable structures are bundles of bars that can be folded and unfolded by rotating around internal ball joints. They are structures with considerable potential, as they can be transported in a compact manner and deployed to form an enclosure that can be used in various useful applications. This capacity is of particular interest in the case of emergency buildings, which is the line of research on which this work is based.

The first deployable bar structures were developed by the Spanish architect Emilio Pérez Piñero. He was the first to propose this type of structure and the first to build it. His early death cut short significant developments in this line of research.

The module used by Pérez Piñero is the so-called bundle modulus [1]. It consists of a set of 3 or 4 bars that are articulated laterally on a central pivot. The ends of the bars articulate with other modules to form a spatial grid. Naturally, in order for this grid to be deployable, it is necessary for it to be a mechanism, which in this type of grid implies a high number of degrees of freedom. Once deployed, the appropriate external constraints are applied so that it works as a structure, resisting external loads.

Pérez Piñero was the author of the first large-scale deployable structure to be built, the pavilion for the 25 Years of Peace Exhibition in 1964, which was initially deployed in Madrid and later moved to Barcelona and San Sebastian [2]. The roof was made of sheet metal, which contributed to the rigidity of the whole, so that the bar sections were very slender. The structure was mounted on the ground, including the roof, and was raised to its final position on four-bar columns that were also folded. In addition to this pavilion, he built experimental dome structures with spans of up to 34 m that demonstrated the viability of the system [3]. His designs attracted the attention of NASA for the future construction of lunar shelters, although the subject was not developed [4].

Research on deployable structures was taken up again in the 1980 s and 1990 s with the works of Escrig et al. 1988, 1999 [5,6]; Pérez-Valcárcel et al. 1987, 1995 [7,8]; Gantes et al. 1991 [9] or Hernández and Zalewsky 1991, 2005 [10,11]. These researchers, together with many others, analysed in particular the modules formed by pairs of bars that are articulated around an internal through joint in a similar way to that of a scissor, and known as scissor-like elements, (SLEs). These elements can be grouped into three-dimensional modules with a triangular base or a square base. The strong theoretical development of SLE module grids was rarely put into practice. The most notable structure built was the cover of the San Pablo swimming pool in Seville by Escrig, Sánchez

---

* Corresponding author.

and Pérez-Valcárcel [12].

The bundle modulus have not received the same attention. We can cite the works of Pérez-Valcárcel and Escrig [13] on a square module of beams with a central bar that allows the self-folding of a textile cover in both layers of the grid. Martín analysed in detail the geometric and mechanical conditions of the bundle modulus domes, the most exhaustive work on this typology to date [14,15,16]. Recently a number of interesting studies have been carried out, such as that of Akgün et al. which proposes various structural types based on the bundle modulus [17].

In terms of practical achievements, the only proposal that can be cited is that of Pérez-Valcárcel et al. for the Asturias Pavilion at EXPO'92 in Seville [18], a square module with a central bar that was never built. It was covered with three expandable umbrellas of square bundle modules that could be deployed obliquely (Fig. 1).

The original designs by Pérez Piñero were based on a set of bars joined together in a central linkage (Fig. 2). When the grid is opened, this linkage forms a reciprocal support that fixes the assembly in its final position and provides it with rigidity so that the structure can withstand external loads. However, the linkages of the upper and lower layers are simple joints, which means that they do not provide the structure with any rigidity or resistance to bending. These linkages make the axial forces of the bars eccentric so that the joint has a certain tendency to turn. In an attempt to prevent this, Pérez Piñero used broken bars, so that their axes coincide with the axis of the joint. This implies problems of buckling which have already been pointed out by Pérez-Valcárcel et al [19]. In all these studies, as well as those of all the later researchers, it is considered that the joints at the ends of the bars are articulated.

Recent research by the authors suggests another approach to the problem [20]. It is possible to design structures in which the end linkages of the bars also have a reciprocal support, hardly used in deployable structures, but which has been the subject of recent work of great interest.

Reciprocal structures try to solve the problem of covering a span with pieces of smaller dimensions than that, without intermediate supports. The elements of the structure mutually support each other until the desired dimension is reached. These lattices have a good structural functioning according to studies of their resistant behavior [21,22]. It is convenient to design reciprocal structures with redundant connections, to avoid that the failure of a single piece causes the collapse of the whole.

In general, reciprocal structures have been used for roofs such as those based on the system described by Popovič [23]. However, its use in deployable structures is limited. We can cite the proposal by Sánchez, Escrig & Rodríguez for deployable umbrellas [24]. Recently Ramos & Sánchez have published an article on deployable hyperboloid modules of great interest [25].

A promising line of research may consist of combining the advantages of portability in compact packages, typical of deployable structures, and the rigidity provided by reciprocal linkages when deploying the mesh. For this purpose, the use of a new type of extremely simple linkage is proposed, in which the free rotation of the end of the bar is compelled by the action of the other bars that converge at the linkage. The system consists of a hollow, circular or square section to which the bars are fastened laterally, so that when they are opened they rest on each other to form a reciprocal structure (Fig. 3).

With this arrangement, the end linkages of the bars are no longer simple joints, but reach a bending rigidity close to embedding. The structures have less deformation and less bending stress. It is a very simple and economical system, especially useful for emergency buildings, where the spans are not large. It is undoubtedly a novel approach, and so far there is only one patent for the system developed by the authors [20]. A recent article has studied the effectiveness of this type of linkage in deployable structures formed by SLEs, but the system is equally valid for those with bundles [26]. Experimental studies demonstrate the efficacy and strength of these reciprocal knots until failure [27].

According to the available data, no other architectural or civil engineering application of deployable bundle modulus structures with extreme reciprocal linkages has been developed. Until now, deployable bundle modulus structures have always been designed and built with modules connected to each other with articulated linkages. The central linkage forms a reciprocal support, but the rest are simple joints.

The aim of this paper is to discuss the behaviour, both theoretical and experimental, of deployable bundle modulus structures with reciprocal links, in order to obtain an in-depth understanding of their structural behaviour and performance.

The originality of this article focuses on the following four aspects

- A demonstration of the geometric and kinematic feasibility of deployable bundle modulus structures built with reciprocal linkages, and a study of the necessary linkages.
- A study of the mechanical conditions of the bars and their influence on the general behaviour of the structure.
- The proposal of a calculation model that takes into account the effects of reciprocal support and eccentricity on the linkages.
- A theoretical and experimental analysis of this type of structure.

The aim of the study is the structural response of deployable bundle modulus structures with reciprocal links and their practical applications. The reciprocal linkage system allows for the design of deployable structures that are more resistant and less deformable than conventional ones. This implies opening up a relevant line of research for future work.

Following the initial definition, the geometric and compatibility conditions of the reciprocal linkages are analysed (Section 2). The influence of the embedding degree due to the reciprocal support of the linkages is analysed by means of a matrix analysis that takes this effect into account (Section 3). The materials and methods used in the experimental analysis are described (Section 4) and the results obtained (Section 5). The results are provided, including a comparison between the results of the theoretical calculation and those obtained in the tests (Section 6). The conclusions and perspectives are presented in Section 7.
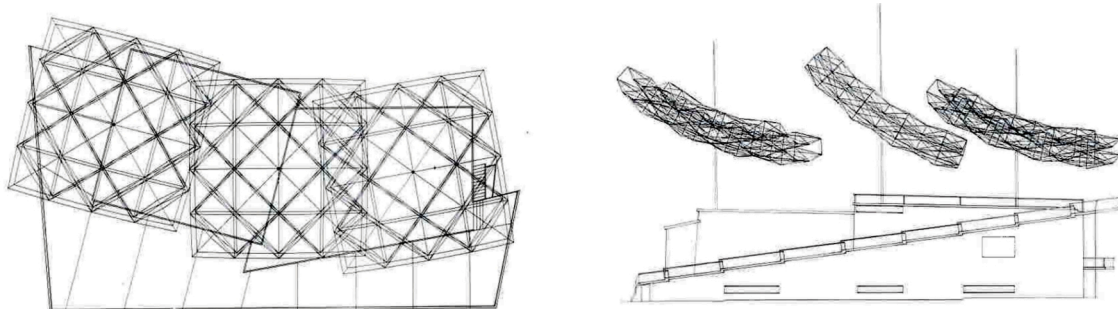

Fig. 1. Design for the Pavilion of Asturias in EXPO'92. Roof plan and west elevation.
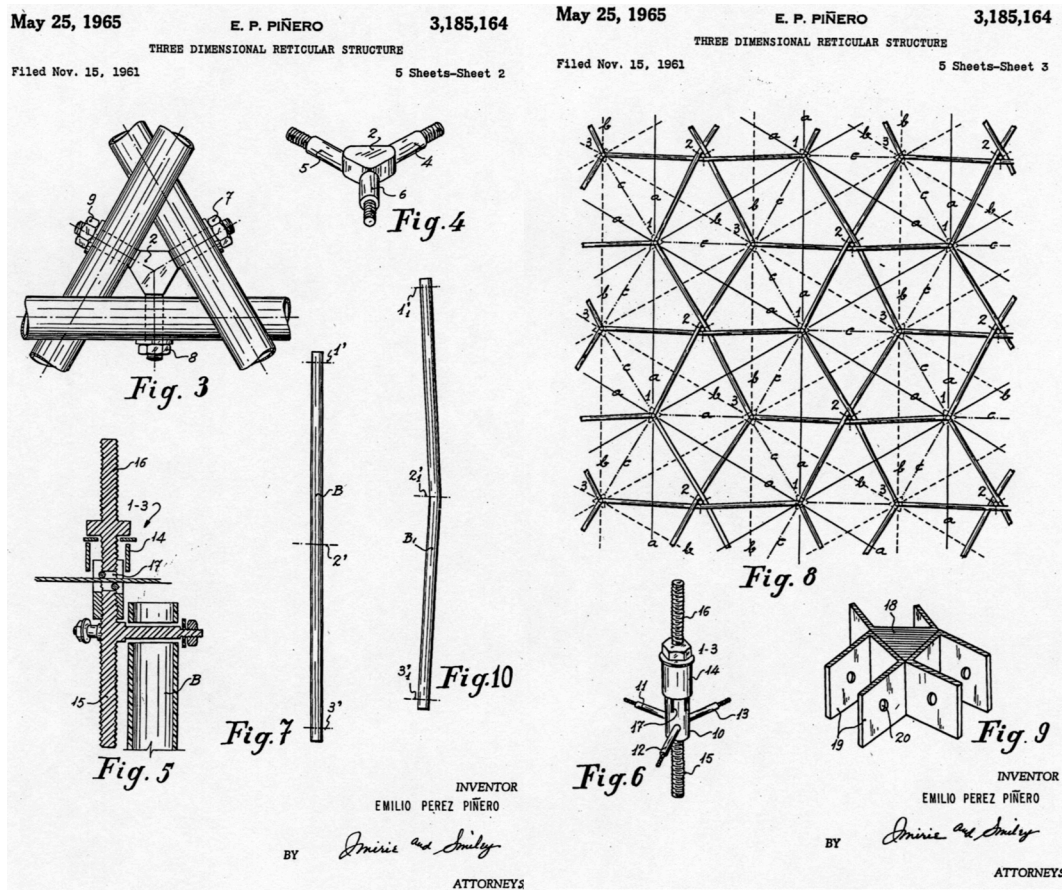
Fig. 2. Bundle and linkage structure from Emilio Pérez Piñero's patent.

Fig. 3. Reciprocal linkages using three and four bars.

2. Characteristics of bundle modulus structures with reciprocal linkages

The bundle modulus offers important advantages. These are deployable structures that can cover an area with fewer bars and links, which means that the machining processes for parts are reduced. In addition, the linkages are particularly simple. In fact, the original linkages patented by Pérez Piñero were made up of a small steel core to which 3 or 4 pivots were welded to articulate the bars (Fig. 2). As an example, a hexagonal grid with a side length of 7.20 m and a module height of 1 m, resolved with four modules per side, would have a total bar length of 262.94 m and would require 133 linkages of the same type. The same grid with blade modules would have a total bar length of 658.91 m and would require 130 links in the upper and lower layers and 160 pins in the blades. In addition, the links of the bundle modulus are simpler and cheaper than most of those used for blade modules (Fig. 4). The same construction system can be used for triangular and square modules by simply modifying the linkage (Fig. 5).

With this data it may appear that beam modulus grids offer better performance than SLE grids, but in reality this is not the case. Bundle modulus grids have some serious drawbacks that have considerably limited their use.

Some are problems of a constructive nature such as those indicated by Pérez Belda [23] and others are design problems such as the limitation of the forms that can be achieved. Flat grids are obtained with bundle modules of equal sections, and if the upper sections are longer
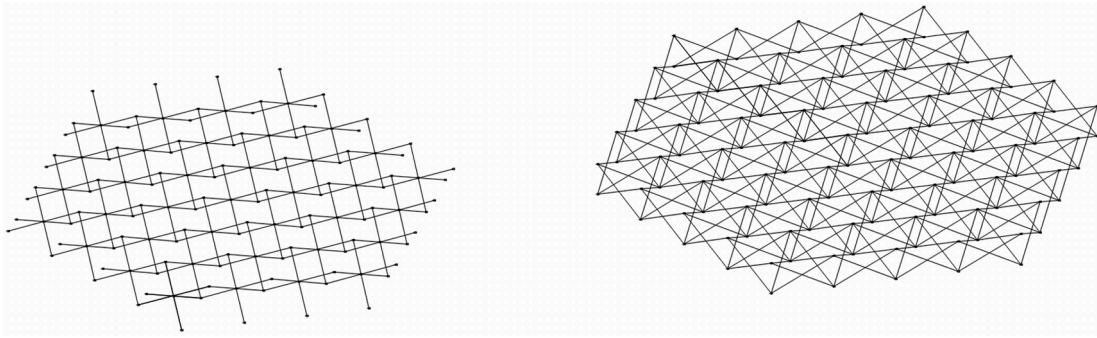
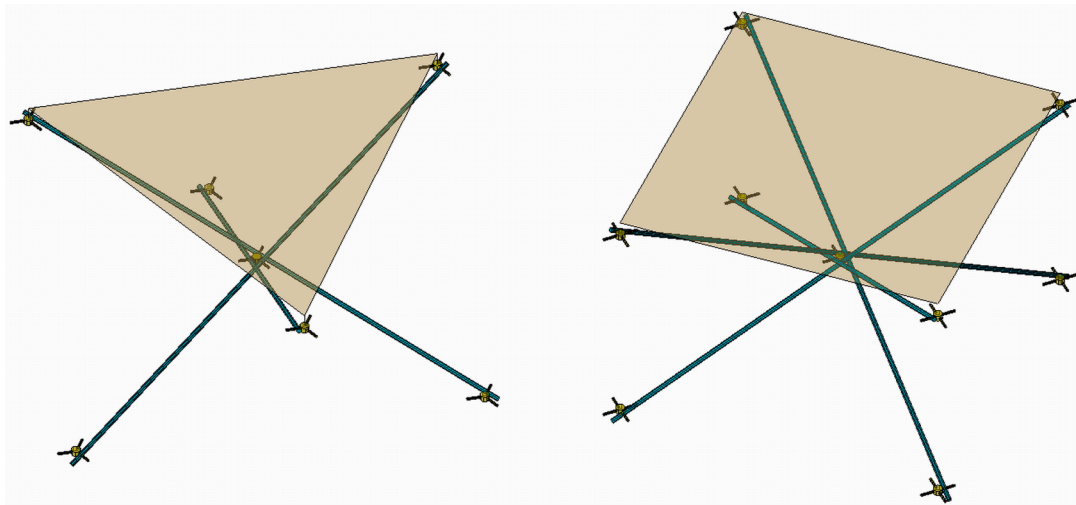**Fig. 4.** Sunshades with bundle modulus and SLEs.

Fig. 5. Triangular and square bundle modulus arrangement.

than the lower ones, domes can be obtained, which are not exactly spherical, but are very close. However, it is not possible to obtain deployable bundle modulus grids if the curvatures are different in both directions, which does not make it possible to design cylindrical domes. Even so, it is possible to design interesting grids, but always with these limitations, which have been extensively analysed by Martín [14,15,16].

Another serious problem with bundle modulus grids is their excessive deformability during deployment. They are mechanisms with a large number of degrees of freedom that do not have elements that can serve as a guide during deployment. The structures formed by SLEs have a certain rigidity in the scissor mechanism itself that causes some limitations in the deployment. Even so, it still presents some problems such as those indicated by Pérez-Valcárcel et al [19], but these effects are more pronounced in the bundle modulus structures. This is one of the main uses of reciprocal linkages. When the structure is deployed, the end linkages tend to curl up, which forces them to occupy their definitive positions, without angular distortions. The models built have demonstrated the effectiveness of this system.

Another problem with bundle modulus grids is the limited stiffness of the edges, which is lower than that of SLE grids. In bundle modulus edge linkages there are two bars, while in SLE grids there are three. The effect is even more pronounced in the corners, where there is only one bundle modulus bar, while in the SLE grid, two bars are joined to the linkage. For this reason it is necessary to provide support systems, which can achieve good results in reducing the deformations of the whole. The most suitable systems consist of supporting various edge modules on vertical posts that allow the links of the upper and lower layers to be fixed in place [28].

However, bundle modulus grids are systematically more deformed

than those formed by SLEs. The proposed system makes it possible to reduce these deformations without introducing additional construction difficulties. The solutions proposed are particularly useful for medium spans, between 10 and 18 m, which is the most suitable range for use in emergency buildings. They are very useful systems for providing communal areas such as canteens, schools, health care centres, etc. The same system can be used for larger spans, but then the structure would be too heavy to be easily transported and assembled. It may be suitable for other types of use, but in emergency buildings, ease of transport and assembly is essential.

The innovation of the proposed system consists in the use of reciprocal linkages formed by three bars in triangular grids and four in square grids. The bars pivot on horizontal axes that extend from the joint that which is formed by a solid or hollow cylinder or prism (Figs. 3 and 5). In the models used in this article, four-bar linkages on a hollow square prism are used. Especially for triangular modules, circular tubular sections can be used, which are very simple and economical. For square based modules, square tubes are more suitable, as they provide a small lateral constraint to the bars, which improves stiffness and facilitates deployment.

The condition of reciprocal support forces the joint to have a minimum dimension that depends on the diameter of the bars and the desired opening angle. As indicated, the bundle modulus grids must have the same angle in both directions. The width of the joint is defined as **D**, and the diameter of the bars that meet in it are defined as **d** (Fig. 6).

The separation between the axis of the bars can be determined by applying the condition that the distance between the two lines that cross each other is **d = 2r**, considering that the bars meet at the point of contact. For square module grids, the angles of the axes of rotation are
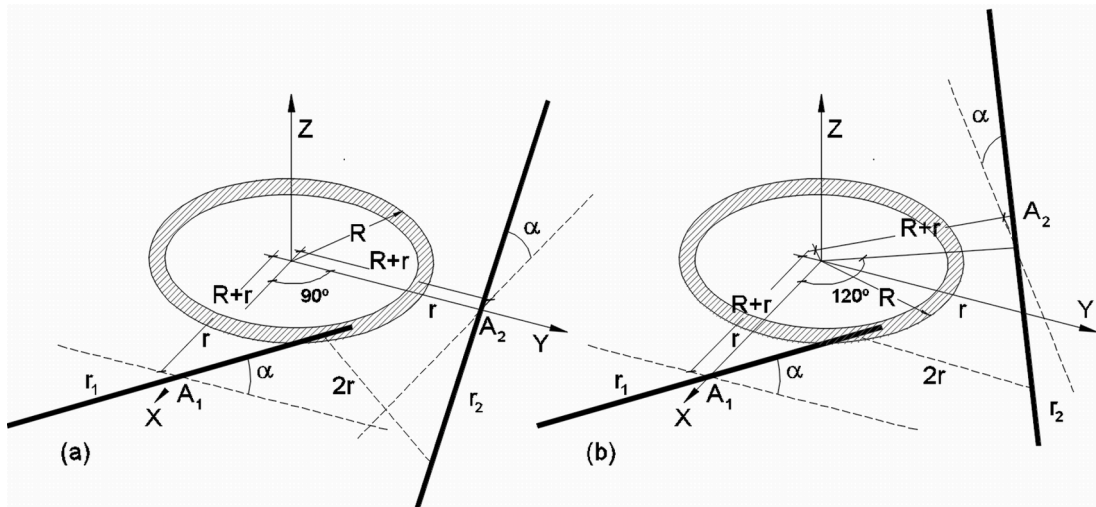
Fig. 6. Geometrical conditions of reciprocal linkages for 4 and 3 bars.

90° and for triangular grids 120°. This implies a major difference between the necessary linkage diameters.

In the case of square module grids the axes of the bars are at a distance from the centre of R + r (Fig. 6a). The straight lines r_1 and r_2, which correspond to the axes of the bars, pass through the points A_1 and A_2 and form an angle α with the reference plane. Their unit vectors are:

$\vec{u}_1 (0, \, cos \, \alpha, \, sen \, \alpha) \; \vec{u}_2 (-cos \, \beta, \, 0, \, sen \, \beta)$

Their passing points are

$A_1 \, (R + r, \, 0, \, 0) \; A_2 \, (0, \, R + r, \, 0)$

The distance between two intersecting lines is the mixed product, divided by the modulus of the vector product. This distance is 2r, considering that the bars meet at the contact point.

$$2r = \frac{\left| A_1A_2 \cdot \vec{u}_1 \cdot \vec{u}_2 \right|}{\left| \vec{u}_1 \times \vec{u}_2 \right|} = \frac{(R + r) \cdot sin \, \alpha}{\sqrt{sin^2 \alpha \, + \, 1}}$$

$$\frac{R}{r} = \frac{D}{d} = \frac{\sqrt{sin^2 \alpha \, + \, 1}}{sin \, \alpha} - 1 \tag{1}$$

In the case of triangular modules, the axes of the bars are also at a distance from the centre of R + r but at an angle of 120° (Fig. 6b). The straight lines r_1 and r_2, that correspond to the axes of the bars pass through the points A_1 and A_2 and form an angle α with the reference plane. Their unit vectors are:

$\vec{u}_1 (0, \, cos \, \alpha, \, sin \, \alpha) \; \vec{u}_2 (-\frac{\sqrt{3}}{2}cos \, \alpha, \, \frac{1}{2} \cdot cos \, \alpha, \, sin \, \alpha)$

Their passing points are

$A_1 \, (R + r, \, 0, \, 0) \; A_2 \left(-\frac{1}{2}(R + r), \, \frac{\sqrt{3}}{2}(R + r), \, 0 \right)$

The distance is defined as in the previous case and must be 2r, since the bars meet at the contact point.

$$2r = \frac{\left| A_1A_2 \cdot \vec{u}_1 \cdot \vec{u}_2 \right|}{\left| \vec{u}_1 \times \vec{u}_2 \right|} = \frac{(R + r) \cdot sin \, \alpha}{\sqrt{sen^2 \alpha \, + \, 0.75}}$$

$$\frac{R}{r} = \frac{D}{d} = \frac{3}{4} \frac{\sqrt{sin^2 \alpha \, + \, 0.75}}{sin \, \alpha} - 1 \tag{2}$$

In order to establish the mechanical conditions of the reciprocal linkages, it is necessary to calculate the distance between the pivot and the point where one bar rests on the other. These distances are:

$$d(A_1, P_1) = \left(\frac{a \, + \, r}{2} \right) \frac{cos\alpha}{1 \, + \, sin^2\alpha}$$

$$d(A_2, P_2) = \left(\frac{a \, + \, r}{2} \right) \frac{cos\alpha}{1 \, + \, sin^2\alpha} \tag{3}$$

The deployable structures that can be obtained with bundle modules are flat and spherical grids. Cylindrical vaults cannot be built with this system.

In the case of flat grids the geometrical ratios are very simple. If **s** is the ground plan dimension of the module and $\mathbf{h_0}$ is the edge following deployment, then it is easy to calculate the angle α and the width **a** required for the linkage (Fig. 7).

$$\alpha = arctan\frac{h_0}{s} \tag{4}$$

In the case of bundle modulus grids, the curved grids form surfaces close to a sphere when deployed, but they do not strictly coincide with it. The module is defined from the lengths of the two sections of the bars $\mathbf{L_1}$, $\mathbf{L_2}$ and from the gap between the upper and lower layers of the grid $\mathbf{h_0}$. Applying the cosine theorem:

$$L_2^2 = L_1^2 + h_0^2 - 2L_1 \cdot h_0 \cdot cos \, \alpha_1 \; ; \; L_1^2 = L_2^2 + h_0^2 - 2L_2 \cdot h_0 \cdot cos \, \alpha_2$$

$$\alpha_1 = arc \, cos \left(\frac{L_1^2 - L_2^2 + h_0^2}{2L_1 \cdot h_0} \right) \; ; \; \alpha_2 = arc \, cos \left(\frac{L_2^2 - L_1^2 + h_0^2}{2L_2 \cdot h_0} \right)$$

$$\alpha = \pi/2 - \alpha_1 \; ; \; \beta = \pi/2 - \alpha_2 \tag{5}$$

As an example and considering a grid formed by Ø40 mm tubes, which is the usual size for emergency modules, we can determine the necessary diameters for the links depending on the angle of the grid. By applying formulas 1 and 2 for square or triangular modules respectively, the size of the linkage can be determined. The relationship between the diameter of the linkage and that of the bar for different angles and types is shown in Table 1.

As can be seen in the table, the size of the linkage is very much conditioned by the angle between the bars. In flat deployable structures the angles are the same in both layers, but in the curved structures, the angles can be very different. As an example we can consider a curved
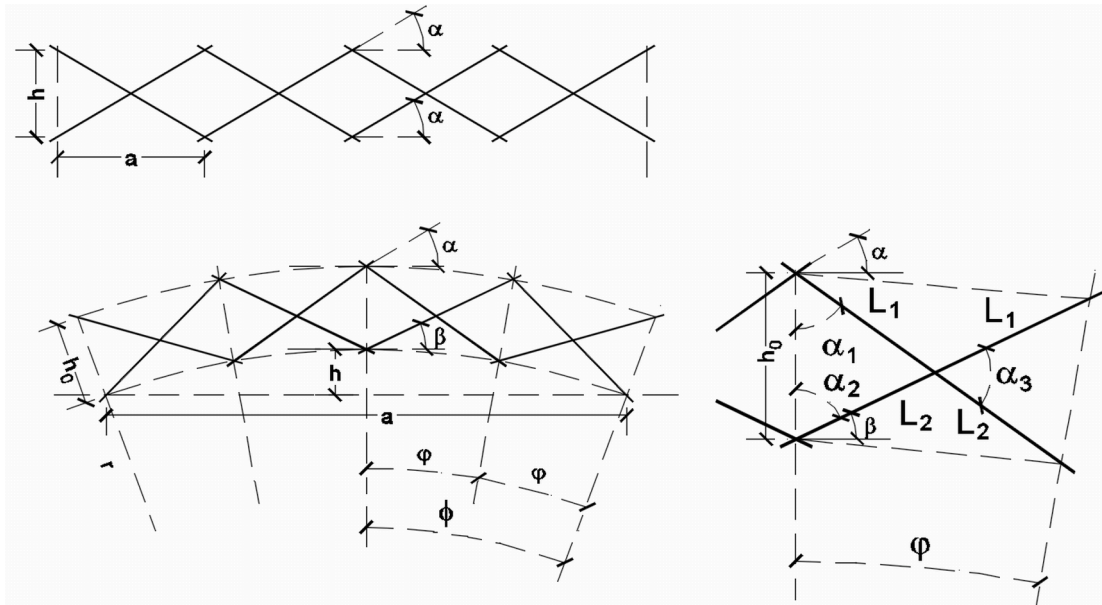
Fig. 7. Geometrical conditions for flat and curved reciprocal grids.

Table 1
Diameters of the linkages according to the grid angle.

Angle αα	d (bar) mm	3 bar linkages		4 bar linkages	
		D/d	D (Linkage) mm	D/d	D (Linkage) mm
15	40	1.62	64.77	1.80	72.19
20	40	1.04	41.67	1.57	62.89
25	40	0.71	28.41	1.39	55.46
30	40	0.50	20.00	1.24	49.44
35	40	0.36	14.33	1.11	44.56

grid with a radius of 15 m, 1 m edge and formed by bars 3 m long and 40 mm in diameter. In this case the angle of the upper layer is 24.79° which requires a linkage of 55.74 mm. On the lower face the angle is 13.97° so the linkage would be 74.38 mm, which may be excessive. A possible solution could be to use reciprocal linkages in the upper layer and articulated linkages in the lower layer.

The most commonly used curved surfaces in deployable beam structures are dome-shaped. The curvature is the same in both directions. The angle of the upper layer is and consequently the diameter of the linkage could be calculated by the previously mentioned formula (2). If the dome has a strong curvature it may be necessary to adjust the dimensions of the bars with decreasing size modules close to the corner. Fig. 8 shows a grid of this type designed by Emilio Martín [14].

3. Computational model

The most suitable calculation model for this type of structure is the Matrix Structural Analysis which has already been proposed in several previous studies [24]. However, for this type of structure it is necessary to take into account two aspects that have been little studied up to now, and which have never been applied to bundle modulus structures, which are the eccentricities in the linkages and the embedding caused by the reciprocal linkages.

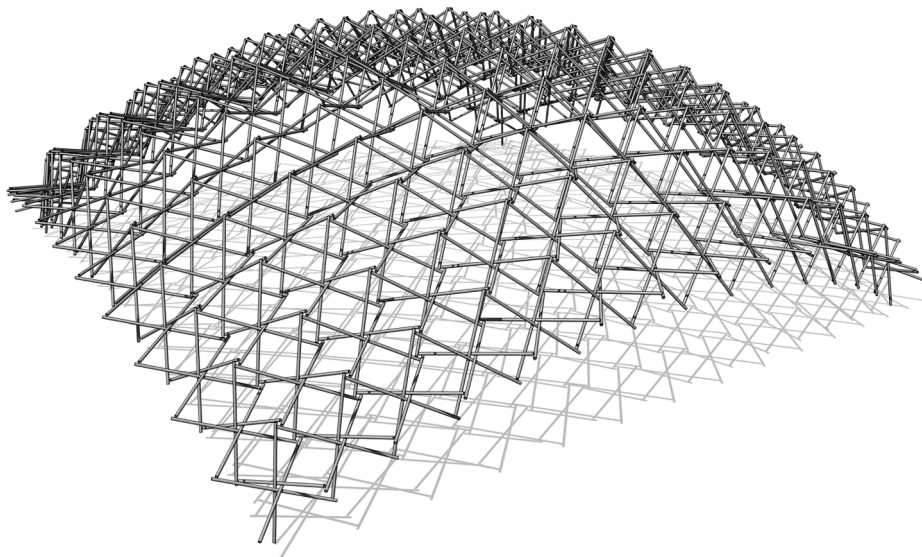In order to correctly consider the equilibrium of the bar in the space,

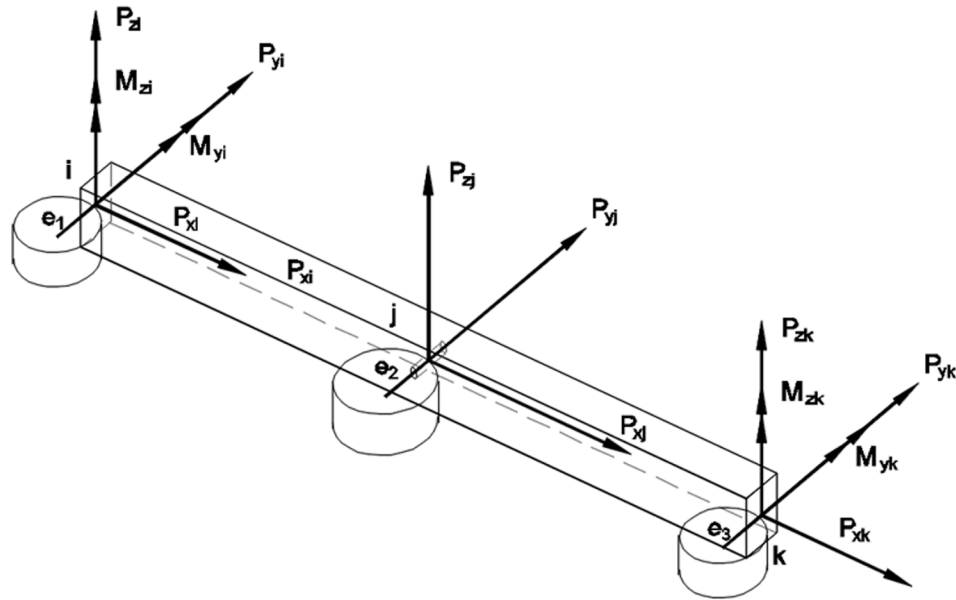**Fig. 8.** Deployable sail dome (courtesy of E. Martín).

Fig. 9. Equilibrium of a bar with three joints in space, with angled linkages at their ends.

it is necessary to take into account that the bars are attached to the linkages with a certain degree of eccentricity (Fig. 9). The eccentricity of each connection point will be the distance between the axis of the linkage and the axis of the bar. It is necessary to take into account that the diameters of the linkages may vary to fit the angles formed by the bars, which vary in the curved grids and the number of bars in the module (Equations (1) and (2)). Therefore, the problem will be formulated assuming that the three eccentricities are different. These eccentricities only affect the deflections in the direction of the y-axis, since on the z-axis the loads and reactions are centred. However, for the bending in the z-axis direction, the reciprocal linkages at the ends of the bars cause some bending moments of reaction at the ends of the bars, which are defined by the embedding degree of the bars.

Considering the equilibrium equation of the bar for the bending moments on the y and z axes, we obtain the following (Fig. 10).

For displacements in the direction of the axis and the reactions at the ends, the axial forces and bending moments are calculated as follows:

$$R_1 = \frac{P \cdot L_2}{L} - \frac{N_1 \cdot (e_1 - e_3) - N_2 \cdot (e_2 - e_3)}{L}$$
$$R_2 = \frac{P \cdot L_1}{L} + \frac{N_1 \cdot (e_1 - e_3) - N_2 \cdot (e_2 - e_3)}{L}$$

(6)

As an energy calculation is to be made, it is more convenient to calculate the forces in each section separately and also to integrate them separately. The total elastic energy will be the partial sum.

The stresses in each of the sections of the bar will be:

Section1

$$N = N_1$$
$$M_{1z} = \frac{P_{yj} \cdot l_2 - N_1 \cdot e_1 - e_3 + N_2 \cdot e_2 - e_3}{L} \cdot x_1 + N_1 \cdot e_1$$
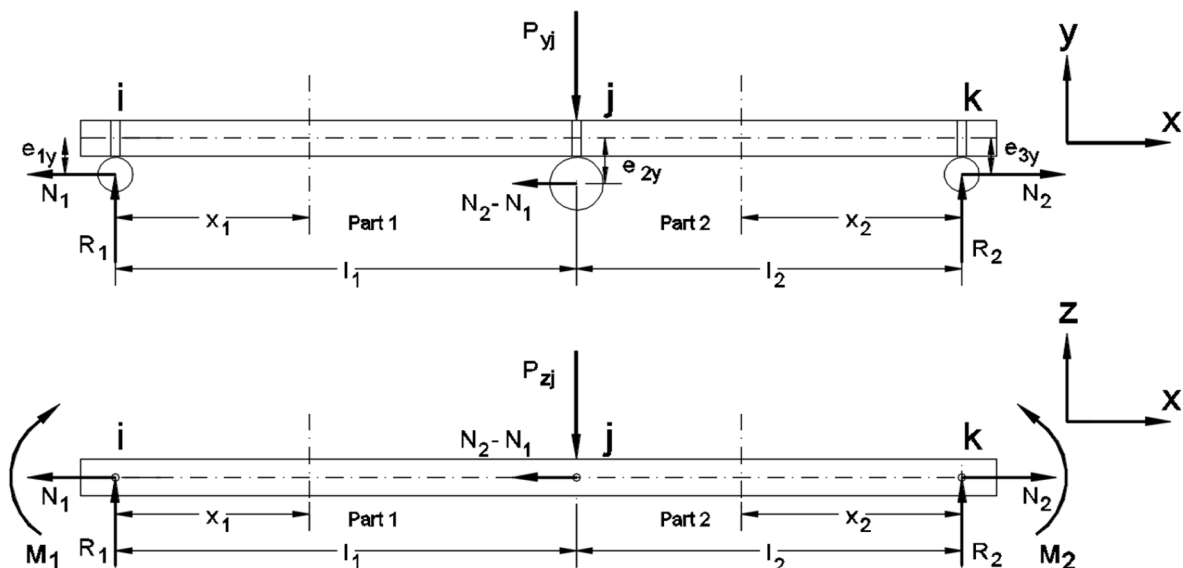

Fig. 10. Equilibrium of the bar on the y and z axes.

Section2 (7)

$$N = N_1$$

$$M_{2z} = \frac{P_{yj} \cdot l_1 + N_1 \cdot e_1 - e_3 - N_2 \cdot e_2 - e_3}{L} \cdot x_2 + N_2 \cdot e_2$$

The condition of reciprocal connection causes bending moments to appear at the ends of the bars, which only affect bending along the z-axis, since in the direction of the y-axis there is no reciprocal support.

In the structures with reciprocal linkages the bar rests at its end on the pin that attaches it to the linkage and on the adjacent bar. The structure is shown in Fig. 11, which makes it easy to calculate the stiffness and the embedding factor using Mohr's theorems. To do this we consider that we have a bar that rests on the pin and with a reciprocal support on another of the bars of the linkage. We consider the bending of the support bar to be negligible, since it occurs very close to the linkage. We use **e** to refer to the distance from the pin to the support point on the adjacent bar (equation (3)) and **L** the length of the bar section (Fig. 11).

Applying this condition, the embedding degree will be:

$$g_e = \frac{L}{L + e}$$ (8)

The value of e (the distance between the pivot axis and the support point of one bar on the next) is defined by the geometrical conditions of the linkage and the bar, as indicated in equation (3). With this value it is possible to calculate the stiffness and the embedding degree of the bar. With the usual proportions in deployable structures, the angled end can be considered almost completely embedded, but the calculation program used makes it possible to consider the real embedding degree of each bar.

For displacements in the direction of the z-axis the forces on each of the bar sections will be:

$$\text{Section 1 } M_{1y} = \frac{P_{zj} \cdot l_2}{L} \cdot x_1 - g_1 \cdot \frac{P_{zj} \cdot l_1 \cdot l_2}{L}$$

$$\text{Section 2 } M_{2y} = \frac{P_{zj} \cdot l_1}{L} \cdot x_2 - g_2 \cdot \frac{P_{zj} \cdot l_1 \cdot l_2}{L}$$ (9)

The effect of the eccentricity of the linkages does not permit a direct formulation of the stiffness matrix of the bar in local coordinates. Instead, it is relatively simple to obtain a flexibility matrix, which can then be inverted to obtain the stiffness matrix.

To do so, it is quite appropriate to consider the flexibility matrix in terms of stresses (axial stresses and bending moments) and not in terms of forces (forces and moments). This makes it possible to formulate 4x4 flexibility matrices instead of 9x9, which means considerable operational savings in matrix inversion operations. However, a slightly more complicated compatibility matrix has to be formulated, but this is a problem that has already been solved for some time [30].

The flexibility matrix can be obtained by formulating the elastic energy of the system and then applying Castigliano's theorem. The deformation energy of the bar will be:

$$W = \frac{1}{2} \cdot \int_0^L \left(\frac{M_y^2}{E \cdot I_y} + \frac{M_z^2}{E \cdot I_z} + \frac{k \cdot V^2}{G \cdot A} + \frac{N^2}{E \cdot A} \right) \cdot ds$$ (10)

If, as is customary, the effect of the energy produced by the shear is disregarded, the displacements can be obtained by differentiating the elastic energy with respect to the appropriate forces as follows:
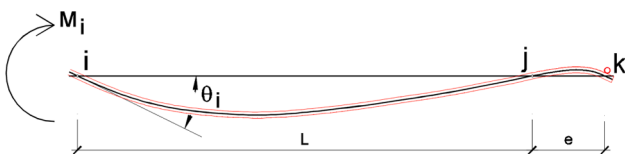

Fig. 11. Stiffness of the bar with reciprocal linkages.

$$u_1 = \int_0^L \left(\frac{N}{E \cdot A} \cdot \frac{\partial N}{\partial N_1} + \frac{M_y}{E \cdot I_y} \cdot \frac{\partial M_y}{\partial N_1} + \frac{M_z}{E \cdot I_z} \cdot \frac{\partial M_z}{\partial N_1} \right) \cdot ds$$

$$u_2 = \int_0^L \left(\frac{N}{E \cdot A} \cdot \frac{\partial N}{\partial N_2} + \frac{M_y}{E \cdot I_y} \cdot \frac{\partial M_y}{\partial N_2} + \frac{M_z}{E \cdot I_z} \cdot \frac{\partial M_z}{\partial N_2} \right) \cdot ds$$

$$v = \int_0^L \left(\frac{N}{E \cdot A} \cdot \frac{\partial N}{\partial P_{yj}} + \frac{M_y}{E \cdot I_y} \cdot \frac{\partial M_y}{\partial P_{yj}} + \frac{M_z}{E \cdot I_z} \cdot \frac{\partial M_z}{\partial P_{yj}} \right) \cdot ds$$

$$w = \int_0^L \left(\frac{N}{E \cdot A} \cdot \frac{\partial N}{\partial P_{zj}} + \frac{M_y}{E \cdot I_y} \cdot \frac{\partial M_y}{\partial P_{zj}} + \frac{M_z}{E \cdot I_z} \cdot \frac{\partial M_z}{\partial P_{zj}} \right) \cdot ds$$ (11)

By solving these integrals we can obtain a flexibility matrix as follows:

$$\begin{pmatrix} u_1 \\ u_2 \\ v \\ w \end{pmatrix} = \begin{pmatrix} f_{11} & f_{12} & f_{13} & f_{14} \\ f_{21} & f_{22} & f_{23} & f_{24} \\ f_{31} & f_{32} & f_{33} & f_{34} \\ f_{41} & f_{42} & f_{43} & f_{44} \end{pmatrix} \cdot \begin{pmatrix} N_1 \\ N_2 \\ P_{yj} \\ P_{zj} \end{pmatrix} \quad \widetilde{U} = \widetilde{F} \cdot \widetilde{L}$$ (12)

In which the values of f_{ij} are defined as

$$f_{11} = \frac{l_1}{E \cdot A} + \frac{e_{1y}^2 \cdot l_1}{EI_y} - \frac{e_{1y} \cdot (e_{1y} - e_{3y}) \cdot l_1^2}{L \cdot EI_y} + \frac{(e_{1y} - e_{3y})^2 \cdot (l_1^3 + l_2^3)}{3L^2 \cdot EI_y}$$

$$f_{12} = f_{21} = \frac{e_{1y} \cdot (e_{2y} - e_{3y}) \cdot l_1^2}{2L \cdot EI_y} + \frac{e_{2y} \cdot (e_{1y} - e_{3y}) \cdot l_2^2}{2L \cdot EI_y} - \frac{(e_{1y} - e_{3y})(e_{2y} - e_{3y}) \cdot (l_1^3 + l_2^3)}{3L^2 \cdot EI_y}$$

$$f_{13} = f_{31} = \frac{e_{1y} \cdot l_1^2 \cdot l_2}{2L \cdot EI_y} - \frac{(e_{1y} - e_{3y})(l_1^3 l_2 - l_1 l_2^3)}{3L^2 \cdot EI_y}$$

$$f_{14} = f_{41} = 0 \quad f_{22} = \frac{l_2}{E \cdot A} + \frac{e_{2y}^2 \cdot l_1}{EI_y} - \frac{e_{2y} \cdot (e_{2y} - e_{3y}) \cdot l_2^2}{L \cdot EI_y} + \frac{(e_{2y} - e_{3y})^2 (l_1^3 + l_2^3)}{3L^2 \cdot EI_y}$$

$$f_{23} = f_{32} = \frac{e_{2y} \cdot l_1 \cdot l_2^2}{2L \cdot EI_y} + \frac{(e_{2y} - e_{3y})(l_1^3 l_2 - l_1 l_2^3)}{3L^2 \cdot EI_y}$$

$$f_{24} = f_{42} = 0$$

$$f_{33} = \frac{l_1^2 l_2^2}{3L \cdot EI_y}; f_{34} = f_{43} = 0$$

$$f_{44} = \frac{l_1^2 l_2^3 + l_1^3 l_2^2}{3L^2 \cdot EI_z} - g_1 \cdot \frac{l_1^2 l_2^3}{L^2 \cdot EI_z} - g_2 \cdot \frac{l_1^3 l_2^2}{L^2 \cdot EI_z} - g_1^2 \cdot \frac{l_1^2 l_2^3}{L^2 \cdot EI_z} - g_2^2 \cdot \frac{l_1^3 l_2^2}{L^2 \cdot EI_z}$$ (13)

And by matrix inversion, the stiffness matrix of the bar can be obtained

$$\widetilde{L} = \widetilde{F}^{-1} \cdot \widetilde{U} \Rightarrow \widetilde{K} = \widetilde{F}^{-1}$$

$$\begin{pmatrix} N_1 \\ N_2 \\ P_1 \\ P_2 \end{pmatrix} = \begin{pmatrix} f_{11} & f_{12} & f_{13} & f_{14} \\ f_{21} & f_{22} & f_{23} & f_{24} \\ f_{31} & f_{32} & f_{33} & f_{34} \\ f_{41} & f_{42} & f_{43} & f_{44} \end{pmatrix}^{-1} \cdot \begin{pmatrix} u_1 \\ u_2 \\ v \\ w \end{pmatrix}$$

$$= \begin{pmatrix} k_{11} & k_{12} & k_{13} & k_{14} \\ k_{21} & k_{22} & k_{23} & k_{24} \\ k_{31} & k_{32} & k_{33} & k_{34} \\ k_{41} & k_{42} & k_{43} & k_{44} \end{pmatrix} \cdot \begin{pmatrix} u_1 \\ u_2 \\ v \\ w \end{pmatrix}$$ (14)

The transformation matrix is similar to the one obtained without considering the eccentricities in the linkages, since the orientation of the local axes does not vary for this reason. It has already been widely studied in previous works [24]. However, the definition of the local axes needs to be clarified. In bundle modules, the reference system is determined by the plane formed by the axis of the bar and the pivot that serves as the axis of rotation in the central joint. The unit vector **a** in the Fig. 12 is taken as a reference, which corresponds to the sum of the unit vectors of the all bars of the linkage. The orientation of the local axes will be:

axis (cos α₁, cos β₁, cos γ₁) → bar direction

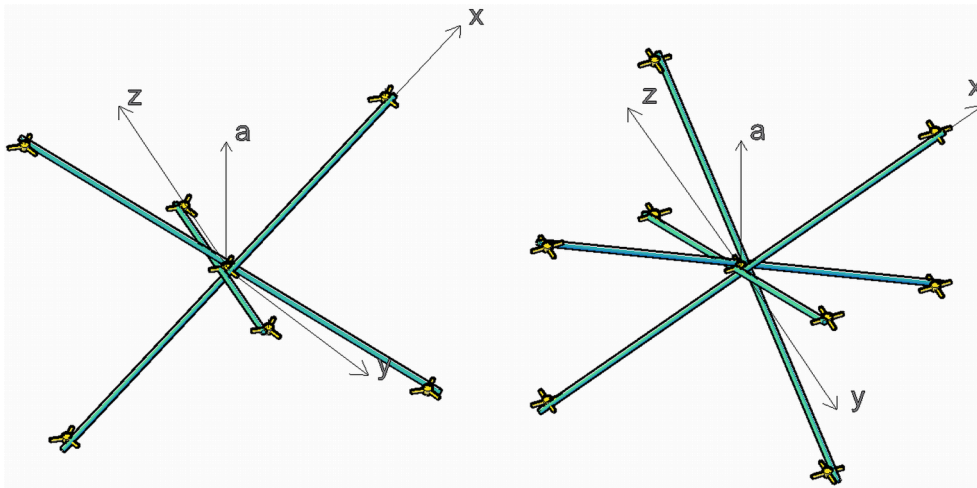Y axis (cos α₂, cos β₂, cos γ₂) → pivot direction. This can be obtained
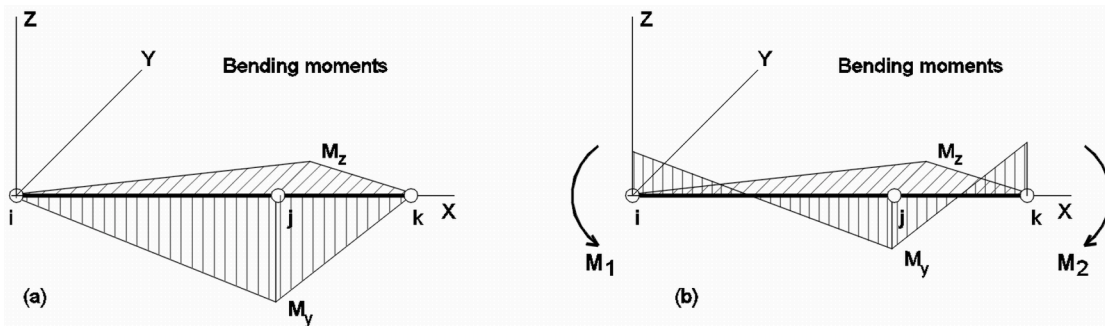
Fig. 12. Definition of the local axes.

Fig. 13. Diagrams of bending moments for articulated and reciprocal linkages.

by the cross product of the unit vector of the bar and the vector **a**.

Z axis (cos α_3, cos β_3, cos γ_3) → direction perpendicular to the × and y axis. It is obtained by the cross product of both unitary vectors.

The transformation equation will be:

$$\widetilde{U} = \widetilde{A} \cdot \widetilde{X}$$

software, which allows for the matrix calculation of bar structures applying these conditions. To validate these calculations, we built the models that are analysed in the section 4.3.

One important advantage of this type of linkage is that it reduces the bending moments on the bar. Fig. 13a shows the bending moments on a bar with its hinged ends and Fig. 13b shows the bending moments with

$$\underbrace{\begin{pmatrix} u_1 \\ u_2 \\ v \\ w \end{pmatrix}}_{\widetilde{U}} = \underbrace{\begin{pmatrix} -cos\alpha_1 & -cos\beta_1 & -cos\gamma_1 & cos\alpha_1 & cos\beta_1 & cos\gamma_1 & 0 & 0 & 0 \\ 0 & 0 & 0 & -cos\alpha_1 & -cos\beta_1 & -cos\gamma_1 & cos\alpha_1 & cos\beta_1 & cos\gamma_1 \\ -\frac{l_2cos\alpha_2}{l} & -\frac{l_2cos\beta_2}{l} & -\frac{l_2cos\gamma_2}{l} & cos\alpha_2 & cos\beta_2 & cos\gamma_2 & -\frac{l_1cos\alpha_2}{l} & \frac{l_1cos\beta_2}{l} & \frac{l_1cos\gamma_2}{l} \\ -\frac{l_2cos\alpha_3}{l} & -\frac{l_2cos\beta_3}{l} & -\frac{l_2cos\gamma_3}{l} & cos\alpha_3 & cos\beta_3 & cos\gamma_3 & -\frac{l_1cos\alpha_3}{l} & \frac{l_1cos\beta_3}{l} & \frac{l_1cos\gamma_3}{l} \end{pmatrix}}_{\widetilde{A}} \cdot \underbrace{\begin{pmatrix} x_1 \\ y_1 \\ z_1 \\ x_2 \\ y_2 \\ z_2 \\ x_3 \\ y_3 \\ z_3 \end{pmatrix}}_{\widetilde{X}} \quad (15)$$

By applying the equilibrium equation, the system of equations to be solved to calculate the stresses and displacements of the structure is obtained.

$$\widetilde{P}' = \left(\widetilde{A}^* \cdot \widetilde{K} \cdot \widetilde{A} \right) \cdot \widetilde{d}' \quad (16)$$

These parameters are entered in the Despleg 19.1 calculation

reciprocal linkages. The most important moments occur in the vertical z direction, which is the direction in which the reciprocal linkages work. The moments Mz do not vary, but in the vertical direction the embedding degree at the ends decreases the moments My almost by half. It is precisely these bending moments that are the most unfavourable stresses in deployable structures.
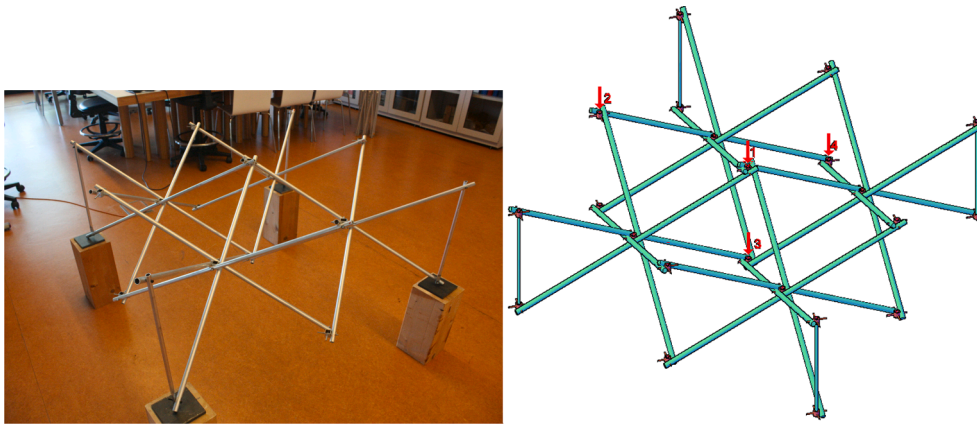
Fig. 14. Bundle modulus model with reciprocal linkages and calculation model scheme.

4. Materials and methods

4.1. Test elements

In order to be able to compare the effectiveness of the reciprocal linkages at the ends of the bars, a series of tests were carried out on two structures with the same dimensions and bar sections. In one of them, the end linkages were simply articulated and in the other, the bars were supported around the linkages forming a reciprocal linkage. Fig. 14 shows the model of the reciprocal linkages and its design, indicating the position of the measurement sensors.

The models built were flat 2x2 module grids. The reason for choosing this type of structure is that it is a particularly deformable grid, so it is very suitable for checking its movements. In the tests, loading–unloading cycles were carried out to check its linear behaviour and the results were compared with those predicted in the calculation programme.

4.2. Materials

The bars of the test model were type 6060- (aluminium-magnesium-silicon) T5 aluminium tubes of Ø16 mm and 1.9 mm thickness. They have a specific weight of 2700 kN/m3, an elastic module of 69500 N/mm2, an elastic limit of 185 N/mm2 and a breaking load of 220 N/mm2. For the corner bracing bars of the grids, Ø13 mm and 1.5 mm thick aluminium tubes of the same material were used.

The linkages were made of hollow aluminium tube sections (SHS) of the same quality, with 20 mm sides, 1 mm thickness and a height of 20 mm. The pivots were made of 4 mm threaded steel rods that were welded in the middle. The screws and threaded rods were made of 5.6 quality steel according to ISO 898–1. They have an elastic module of 200,000 N/mm2, an elastic limit of 300 N/mm2 and a breaking load of 500 N/mm2 with an elongation of 20%.

4.3. Manufacturing of the elements

The models were built to 1:4 scale. As they were flat grids, the lengths of the bars were equal and the inner linkage was at the central point of the bar. The angles were the same in all the points of the grid, both in the upper and lower linkages, so the linkage was always the same size. This made construction easier and minimised any possible mismatches during assembly. In fact, it was possible to verify that reciprocal support existed in all the linkages.

The two models tested were comprised of four square modules. Each of them was made of bundles of 4 bars that were arranged around the central linkage. In both cases the lengths of the two bar sections were 470 mm between the pivots of the connections. In the reciprocal linkages model, the bar extended by 30 mm from the end pivot axis, meaning the total length of the bar was 1000 mm. In the articulated

linkages model, the bar was extended by 10 mm, making the total length of the bar 960 mm. The height of the grid was 427 mm and the angle of the bars was 27.20°. This means that the ratio between the diameters of the linkage and the bar is 1.3164. The diameter of the linkage required is 21.06 mm. The linkage was adjusted to the precise diameter with two 0.5 mm washers, ensuring that all of the bars were reciprocally supported.

In bundle modulus grids, one particularly delicate point is the corner. If it is supported at this point, the reaction can only be resisted the bending of the end section of the bar, which is extremely ineffective. In the models tested, bracing bars were placed in the corners to at least distribute the reaction between the two bars (Fig. 14). In practice, these grids are usually supported at several points, but for the tests it was considered a suitable solution.

The models were tested at the School of Architecture's structures laboratory in A Coruña, which has a test bench designed for this type of structure. Five 10 kgf (98.1 N) loads were applied to the upper central linkage and central linkages of each module. As the aim is to be able to compare the theoretical and experimental results, the loads can be placed wherever required, and this is a suitable position so that the loads do not interfere with the sensors. The displacements were measured with Schreiber Sm407.100.2.T inductive displacement sensors with linearity < 0.25% and deviation < 0.01%/°C at the central points of the grid. The data collection was completed with Y103 digital extensometers with an accuracy of ± 0.1 mm in border points.

The models were supported by four wooden blocks with polypropylene panels that allowed the supports to slide. Friction is minimal, so the only effective constraint is vertical displacement. This is the most unfavourable situation for the grid. In real grids there are constraints on horizontal movements, which reduces vertical displacements. In order to verify the greater effectiveness of the reciprocal linkages against vertical displacements, it is advisable to design the model for a particularly unfavourable situation.

4.4. Organisation of the tests

In all tests, a preload step was first performed to adjust the linkages. This is a very important aspect of deployable structures. As they are mobile structures, the joints and linkages need to have a certain tolerance to allow for movements during deployment. When entering into load, the structure readjusts and has a certain initial displacement. After unloading this previous step, the structure largely maintains this adjustment position, although there is a slight recovery. When the next loading step is carried out, the structure deforms according to the applied load. This is essential if the calculation methods are to be validated with the experimental results. Shifts in the adjustment would distort the measured results and prevent their effective comparison.

Table 2
Data for the calculation of the reciprocal support grids tested.

Angle α	D/d	d (bar) mm	D (Linkage) mm	d(A$_1$,P$_1$) mm	d(A$_2$,P$_2$) mm	L	G$_{e1}$
27.2	1.3164	16	21.06	13.52	13.52	470.00	97.20%

Table 3
Results of theoretical calculations. 2x2 module grid tested.

	Displacements mm				Stress MPa	
	Point 1	Point 2	Point 3	Point 4	Bar 1	Bar 2
Artic. linkages	29.64	29.61	17.35	17.33	124.40	119.40
Recipr. linkages	24.98	24.96	16.33	16.30	107.80	103.50
Improvement %	118.65	118.63	106.25	106.32	115.40	115.36

5. Results

5.1. Theoretical model

The calculation software used was Despleg19.1, developed by the authors using the structural analysis matrix with the settings indicated in section 3. In the case of the grid with reciprocal linkages, the programme assigns to the end linkages of the bars and to the central linkages of the modules an embedding degree that the programme calculates as a function of the lengths of the bars and the distances of reciprocal support. In the calculations performed for the grid of hinged linkages, it is considered that the bars lack stiffness at their ends (Table 2).

In the tested reciprocal linkages modules the embedding degree is 97.20%. In the case of linkages with four bars, this degree of installation applies to all the bars. In the model tested, it only occurs in the upper and lower central linkages. In the case of the edge and corner linkages, it can only be applied to the bars that support each other. The ends of the bars that are not supported must be considered with a 0% embedding degree. In the calculation of the grid with hinged linkages, the embedding degree is always 0%.

The constraints are applied so as to consider that the model is simply supported and vertical movement is only prevented at the lower linkages

of the four corners. The loads are those of the real model and the results refer to the application points of the sensors.

The last line shows the percentage improvement between the values calculated for the grid with reciprocal linkages and the grid with articulated linkages (Table 3).

Although the improvement is evident, the percentages are not very high. It should be noted that the model calculated and tested consists of only four modules. This means that only the two central linkages have fully effective mutual support. In order to appreciate the advantages of the proposed linkage, several calculations were performed with larger structures, which allowed the performance of the linkage to be tested. For this purpose, the structure shown in Fig. 15 was calculated, consisting of 16 modules 2 m wide and with an edge of 1 m, covering an area of 8.00x8.00 m. The bars are 3 m long, made up of 65.3 aluminium tubes of the same type used in the tests. It is considered to be supported on two opposite edges and the loads are those foreseen in EC-1 [31]. The table shows the displacements at the central points of the grid (30, 31), at the central points of the edge (25, 26) and the stresses on the corner module bars, those subject to the greatest stresses (1, 2) and the central module bars of the grid (93,94). The maximum stresses have been calculated, considering the axial force and the bending moment in the three most unfavourable positions: The central one where the bending moment is maximum and the two extremes in which the bending moment produced by the reciprocal support must be considered (Table 4).

5.2. Experimental results

The tests were carried out with the loads arranged in the linkages indicated above and with the displacement sensors at the points indicated in Fig. 14. A progressive load was applied for about 5 s. The load was maintained for a period sufficient to stabilise the displacements
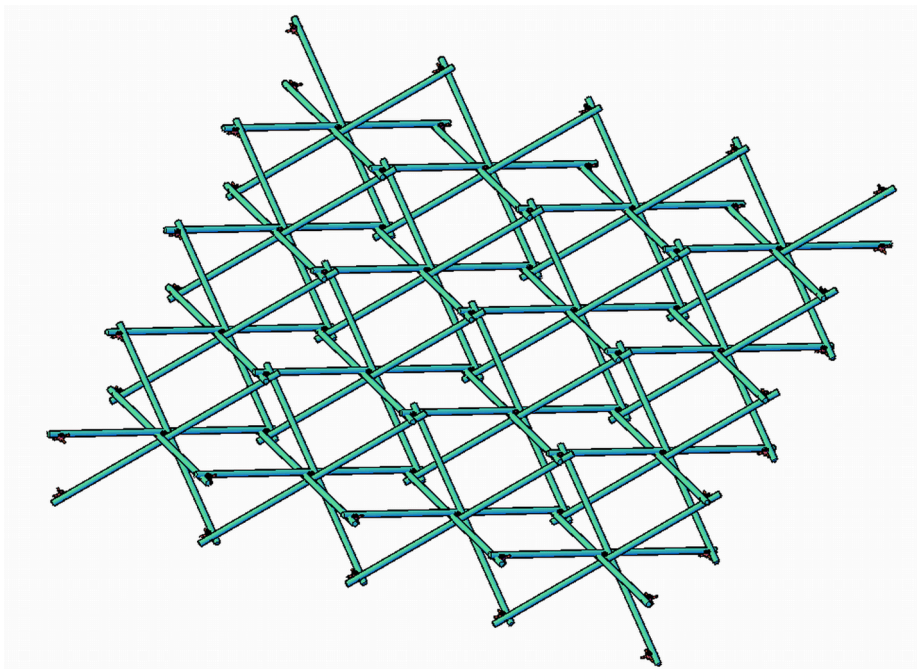

Fig. 15. Structure with an 8x8 m grid.

Table 4
Theoretical results: 8x8 m mesh.

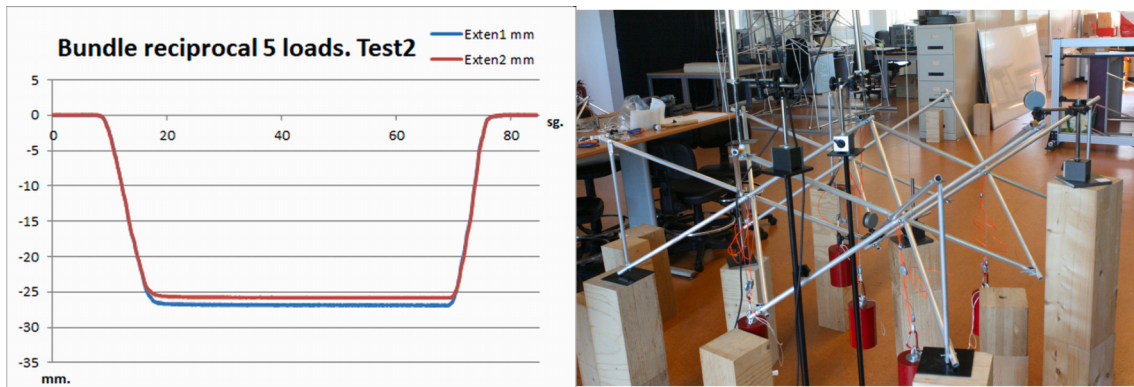|	Displacements mm				Stress MPa			
	Point 30	Point 31	Point 25	Point 26	Bar 1	Bar 2	Bar 93	Bar 94
Artic. linkages	240.10	363.60	421.60	480.00	46.90	275.50	240.90	156.10
Recipr. linkages	109.90	167.50	185.20	224.30	54.60	133.10	156.10	97.60
Increase %	−54.23	−53.93	−56.07	−53.27	16.42	−51.69	−35.20	−37.48

Fig. 16. Displacements of test for grids with reciprocal linkages and corner bars.
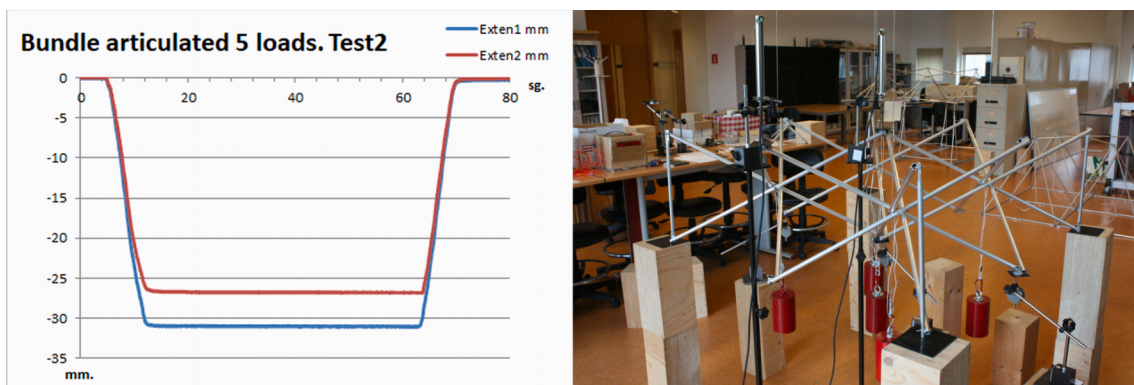

Fig. 17. Grid test displacements with articulated linkages and corner bars.

Table 5
Grid movements with reciprocal and articulated linkages.

	Reciprocal linkages				Articulated linkages			
	Displacements mm				Displacements mm			
Points	1	2	3	4	1	2	3	4
Test 1	26.88	25.05	23.75	18.57	30.91	26.73	23.09	21.16
Test 2	26.80	25.78	23.61	20.94	30.76	26.74	23.37	21.16

Table 6
Comparative analysis of measured and calculated values.

	Reciprocal linkages				Articulated linkages			
	Displacements mm				Displacements mm			
Points	1	2	3	4	1	2	3	4
Test 1	26.88	25.05	23.75	18.57	30.91	26.73	23.09	21.16
Test 2	26.80	25.78	23.61	20.94	30.76	26.74	23.37	21.16
Average value	26.84	25.42	23.68	19.76	30.84	26.74	23.23	21.16
Standard dev.	0.06	0.52	0.10	1.68	0.11	0.01	0.20	0.00
Theoretical	24.98	24.96	16.33	16.30	29.64	29.61	17.35	17.33
Test/theor.	1.074	1.018	1.450	1.212	1.040	0.903	1.339	1.221

between 40 and 50 s, and then progressively discharged for 5 s. Two tests were carried out for each of the cases.

5.2.1. Flat grids with reciprocal linkages and corner bracing bars

The model is comprised of 1000 mm bars with a 30 mm reciprocal end from the bolt. The centre distance of the end bolts is 940 mm. The displacements in points 1 and 2 have been measured and recorded with Sm407.100.2.T inductive displacement sensors and in points 3 and 4 with Y103 digital extensometers (Fig. 16).

5.2.2. Flat grids with articulated linkages and corner bracing bars

In this case, the lengths of the bars are 960 mm, leaving a final length from the bolt of 10 mm. The ends rotate freely without support between them. The placement of the sensors and the load pattern is the same as in the previous test (Fig. 17).

In summary, the results of the tests carried out are (Table 5)

6. Discussion

Firstly, the values of the tests carried out will be compared with those foreseen in the theoretical study. Table 6 shows these values, their average, standard deviation and the relationship between the measured values and the theoretical values.

The values measured in the tests show a high degree of coincidence, supported by low values of standard deviation. This coincidence is the reason why it was not considered necessary to carry out a greater number of tests.

In the theoretical calculation model, the effect of the tolerance on the linkages has been considered, as well as an initial displacement of the bars. This is common in deployable structures, since they need to be mechanisms before being fixed in their final position. It is precisely their condition as mechanisms that allow the deployment and folding processes. In the models tested, the diameter of the bolt is 4 mm, while the diameter of the hole in the bar is 4.2 mm. This tolerance of 0.2 mm must be considered in the calculation, and in fact its validity has been proven in numerous tests that were performed previously.

The experimental results practically coincide with the theoretical results in points 1 and 2. However, points 3 and 4 located in the lower layer have greater deviations (Table 3). The pattern of deviation predicted by the theory is that the points in the lower layer have less deformation, since when they come under load the SLEs tend to close. However, in the real grid, it seems that friction and mutual support limit this movement and the deformation is higher than expected.

To test the effectiveness of reciprocal links, it is necessary to compare the results of the grid with articulated and reciprocal linkages. When comparing the experimental results between both types of grids, it can be seen that grids with articulated linkages have displacements in the upper layer that represent an increase of up to 14.88% over the displacements of the grid with reciprocal linkages (Table 7). On the other hand, in the lower layer linkages, the displacements in the central linkage are slightly lower in the case of articulated linkages. This is due to the fact that the assembly of SLEs forms pantograph-shaped squares in which a greater displacement of the upper linkages results in a smaller displacement of the lower linkages. This is not an advantage for the articulated linkage grid. On the contrary, the reciprocal linkages grid has lower maximum displacements and less distortion between them.

This improvement in the displacements occurred in a model in which only the central linkages are reciprocally supported in their entirety. In contrast, in the example given in 5.1 for a 4x4 module grid, with 18 linkages effective at 100%, the improvement in the displacement of the central point is 54.23%, substantially greater. This shows that the efficiency of the system increases considerably by increasing the number of linkages with reciprocal supports on the four bars, as is the case with the grids that will actually be used.

Table 7
Comparison of experimental results.

	Displacements mm			
	Point 1	Point 2	Point 3	Point 4
Reciprocal linkages	26.84	25.42	23.68	19.76
Articulated linkages	30.84	26.74	23.23	21.16
Increase %	14.88	5.19	−1.90	7.11

7. Conclusions

The results obtained show that, for bundle modulus grids, the use of reciprocal links at the ends of the bars is an improvement over the use of articulated linkages. This effect had already been verified by the authors in grids formed by SLEs, and has two advantages. Firstly, the grids are self-stabilising in their final position, and the deployment process is carried out in a more controlled way. In addition, the condition of reciprocity allows a high embedding degree at the ends of the bars, which improves the capacity to withstand bending moments, which are particularly important for the dimensioning of the sections [29].

In bundle modulus structures, the capacity for improvement depends substantially on the number of reciprocal linkages, since by their very nature these structures have a lower number of linkages than SLE structures. In the module tested, with only two fully effective reciprocal links, the improvement in displacement is relatively low: 14.88% in the central linkage, the most favourable. With 18 totally effective linkages, the improvement in the displacement of the central point is 54.23%, substantially higher.

Flat deployable flat structures with articulated linkages offer major advantages, as they are completely regular, and all the bars have the same lengths, which means that they are easier to manufacture and assemble. In fact, the Pérez Piñero structure for "25 years of peace" Pavilion is a flat grid, although it is effectively braced by the rigid panel covering. The reciprocal linkages substantially improve the resistance and rigidity of these structures, making the use of flat grids more efficient. They also allow other types of grids to be designed, such as domes, while maintaining the strength and rigidity benefits of reciprocal linkages.

CRediT authorship contribution statement

J. Pérez-Valcárcel: Conceptualization, Methodology, Software, Validation, Formal analysis, Investigation, Resources, Writing - original draft, Writing - review & editing, Visualization, Supervision, Project administration, Funding acquisition. **M. Muñoz-Vidal:** Conceptualization, Methodology, Software, Validation, Formal analysis, Investigation, Resources, Data curation, Writing - review & editing, Visualization. **F. Suárez-Riestra:** Conceptualization, Methodology, Software, Formal analysis, Investigation, Data curation, Writing - review & editing, Supervision. **Isaac R. López-César:** Conceptualization, Methodology, Validation, Investigation, Resources, Writing - review & editing, Visualization. **M.J. Freire-Tellado:** Conceptualization, Methodology, Investigation, Resources, Writing - review & editing, Supervision.

Declaration of Competing Interest

The authors declare that they have no known competing financial interests or personal relationships that could have appeared to influence the work reported in this paper.

reference BIA2016-79459-R.

References

[1] Pérez Piñero E. Estructura reticular estérea plegable. Spanish Patent 1961;266801.

[2] Pérez Belda E, Pérez Almagro C. 2016. The deployable architecture commemorates the 25 years of peace. 50th Anniversary of Emilio Pérez Piñero's Pavilion EGA Num.28. doi: 10.4995/ega.20166307.

[3] Pérez Piñero E. Estructures reticulées. L'Architecture d'Aujourd'hui. 1968;141: 76–81.

[4] Candela F. En defensa del formalismo. Madrid: Xarait Libros SA; 1985.

[5] Escrig Pallares, F. y Pérez-Valcárcel, J. 1988. Estructuras espaciales desplegables curvas Informes de la Construcción, Vol. 39 n° 393.

[6] Escrig Pallares, F. y Sánchez Sánchez, J. 1999. Estructura plegable de grid para la cubrición de recintos. Patente 2 158 787 A1.

[7] Pérez-Valcárcel J, Escrig F, Martín E, Vázquez JA. "Analysis of expandable domes of squared modulus with self-folding roofing plates". Int. Conference on Spatial Structures: Heritage, present and future IASS. Milán. 1995; Vol 2. pp 551-558.

[8] Pérez-Valcárcel J, Escrig F, Estévez J, Martín E. Large Span Expandable Domes. Int. Conference on Large Span Structures. Toronto. 1992;2:619–30.

[9] Gantes C, Connor JJ, Logcher RD. Combining Numerical Analysis and Engineering Judgement To Design Deployable Structures. Comput Struct 1991;40(2):431–40.

[10] Hernández CH, "New Ideas on Deployable Structures" in Mobile and Rapidly Assembling Structures II. Proceeding of the 2nd MARAS 1996, Seville, Spain, June 17-20, 1996, Escrig & Brebbia, Ed. Computational Mechanics Publications, Southampton, 1996, pp. 63-72.

[11] Hernández C, Zalewski W. Pabellón Itinerante de Exposiciones TaraTara, Estado de Falcón, Venezuela, 2005 (based on the ESTRAN 1 Protoype developed by Hernández Merchán and Zalewski, 1987-2000. IDEC - FAU – UCV.

[12] Escrig F, Pérez-Valcárcel J. Deployable Cover on a Swimming Pool in Seville. "Bulletin of the International Association for Shell and Spatial Structures" 1996;37 (120):39–70.

[13] P.Valcárcel, J.B.; Escrig, F. (1991) Expandable Structures with Self-folding Textile Cover. "International Conference on Mobile and Rapidly Assembled Structures". MARAS'91. Southampton.

[14] Martín E. Estructuras desplegables con módulos de haces y base cuadrangular. (PhD Thesis). Universidade da Coruña. 2001. http://hdl.handle.net/2183/12373.

[15] Martín, E..; P. Valcárcel, J. (2002). Generation of foldable domes formed by bundle modules with quadrangular base. "Bulletin of the International Association for Shell and Spatial Structures". Vol 43. N° 140. pp 133-142.

[16] Martín, E..; P. Valcárcel, J. (2004). Foldable systems based on bundle modules with quadrangular base. "International Journal of Space Structures". Vol. 19. N° 3. pp 155-165.

[17] Akgün Y, Gantes C, Sobek W, Korkmaz K, Kalochairetis K. A novel adaptive spatial scissor-hinge structural mechanism for convertible roofs. Eng Struct 2011;33: 1365–76.

[18] Pérez-Valcárcel, J.B.; Estévez, J.; Martín, E.; Freire, M. (1992). Lema Nao. Concurso de Anteproyectos para el Pabellón del Principado de Asturias. Asturias'92. Oviedo. pp 87-95.

[19] P. Valcárcel, J.; Escrig, F.; Estévez, J.; Martín, E. (1993). Cálculo no lineal de estructuras plegables de barras curvas. "2°Congreso de Métodos Numéricos en Ingeniería". A Coruña. Vol 1. pp 327-336.

[20] Pérez-Valcárcel, J. et al. 2018."Estructura desplegable, edificación y método de construcción de una edificación" Spanish Patent P201831054.

[21] Choo B, Couliette P, Chilton J. Retractable roof using the Reciprocal Frame. Proceedings of IABSE Symposium (Birmingham): Places of assembly and long-span building structures. 1994.

[22] Sánchez J, Escrig F, Rodríguez Mª T. Reciprocal frames designed by Leonardo. An analytical approach. Informes de la Construcción. 2010;Vol. 62, 518:5–14. https:// doi.org/10.3989/ic.09.032.

[23] Popovič Larsen, O. 2014. "Reciprocal Frame (RF) Structures: Real and Exploratory", Kim Williams Books, Turin. Nexus Network Journal. DOI 10.1007/ s00004-014-0181-0.

[24] Sánchez J, Escrig F, Rodríguez Mª T. Reciprocal Tree-like fractal Structures. Nexus Netw J 2014;16:135–50. https://doi.org/10.1007/s00004-014-0182-z.

[25] Ramos-Jaime C, Sánchez-Sánchez J. Hyperboloid Modules for Deployable Structures. Nexus Netw J 2020;22:309–28. https://doi.org/10.1007/s00004-019-00459-y.

[26] Pérez-Valcárcel J, Muñoz-Vidal M, López-César I, Suárez-Riestra F, Freire-Tellado M. A new system of deployable structures with reciprocal linkages for emergency buildings. Journal of Building Engineering 2020;33. https://doi.org/ 10.1016/j.jobe.2020.101609.

[27] J. Pérez-Valcárcel, F. Suárez-Riestra, M. Muñoz-Vidal, I. López-César, M. J. Freire-Tellado 2020. A new reciprocal linkage for expandable emergency structures. Structures. Volume 28, December 2020, 2023-2033. DOI: https://doi.org/ 10.1016/j.istruc.2020.10.008.

[28] Pérez Belda E. (2000). Constructive problems in the deployable structures of Emilio Perez Pinero. International Conference on Mobile and rapidly assembled Structures (MARAS'00). Madrid. pp 23-34.

[29] Pérez-Valcárcel J, Muñoz-Vidal M, Freire Tellado M, López-César I, Suárez-Riestra F. Expandable covers of skew modules for emergency buildings. International Journal of Innovation Engineering and Science Research. 2020;4(5): 38–52.

[30] Pérez-Valcárcel J, Escrig F, Martín E, Domínguez E, Jaureguizar F. "Recent advances in analysis of expandable structures: An improved method". 1998. Int. Conference on Spatial Structures in New and Renovation Projects of Building and Construction IASS. Moscú. Vol 1. pp 192-199.

[31] UNE-EN 1991-1-4: 2018. Eurocode 1. Actions on structures – Part 1-4: General actions – Wind actions.